

A comparative study on the single-scan and multiple-scan techniques in differential scanning calorimetry

Application to the crystallization of the semiconducting $\text{Ge}_{0.13}\text{Sb}_{0.23}\text{Se}_{0.64}$ alloy

J. Vázquez*, D. García-G. Barreda, P.L. López-Aleman, P. Villares, R. Jiménez-Garay

Departamento de Física de la Materia Condensada, Facultad de Ciencias, Universidad de Cádiz, Apartado 40, 11510 Puerto Real (Cádiz), Spain

Received 13 July 2004; received in revised form 20 January 2005; accepted 21 January 2005

Available online 23 February 2005

Abstract

A method has been developed for analysing the evolution with time of the volume fraction transformed and for calculating the kinetic parameters at non-isothermal reactions in materials involving formation and growth of nuclei. By considering the assumptions of extended volume and random nucleation, a general expression of the fraction transformed as a function of time has been obtained in isothermal crystallization processes. Considering the mutual interference of regions growing from separate nuclei the Johnson–Mehl–Avrami equation has been deduced as a particular case. The application of the transformation rate equation to the non-isothermal processes has been carried out under the restriction of a nucleation which takes place early in the transformation and the nucleation frequency is zero thereafter. Under these conditions, the kinetic parameters have been deduced by using the techniques of data analysis of single-scan and multiple-scan. The theoretical method developed has been applied to the glass-crystal transformation kinetics of the semiconducting $\text{Ge}_{0.13}\text{Sb}_{0.23}\text{Se}_{0.64}$ alloy. The kinetic parameters obtained according to both techniques differ by only about 2.5%, which confirms the reliability and accuracy of the single-scan technique when calculating the above-mentioned parameters in non-isothermal transformation processes. The phases at which the above-mentioned semiconducting glass crystallizes after the thermal process have been identified by X-ray diffraction. The diffractogram of the transformed material shows that microcrystallites of Sb_2Se_3 and GeSe are associated with the crystallization process, remaining a residual amorphous matrix.

© 2005 Elsevier B.V. All rights reserved.

PACS: 64.60; 64.70; S7.12; S8.12

Keywords: Semiconducting alloy; Glass-crystal transformation; Differential scanning calorimetry; Extended volume; Single-scan and multiple-scan techniques

1. Introduction

Knowledge of amorphous materials is one of the most active fields of research in the physics of condensed matter today [1]. The great interest in these materials is largely due to their ever increasing applications in modern technology. Their possibilities in the immediate future are huge based

on characteristic properties such as electronic-excitation phenomena, chemical reactivity and inertia, and superconductivity. Therefore, the advances that have been made in physics and chemistry of the quoted materials during the last 40 years have been very appreciated within the research community. A strong theoretical and practical interest in the application of isothermal and non-isothermal experimental analysis techniques to the study of phase transformations has been developed in the last decades. The non-isothermal thermo-analytical techniques have become particularly prevalent for the investigation of the processes of nucleation and growth

* Corresponding author. Tel.: +34 956016323; fax: +34 956016288.

E-mail address: jose.vazquez@uca.es (J. Vázquez).

that occur during transformation of the metastable phases in a glassy alloy as it is heated. These techniques provide rapid information on such parameters as glass transition temperature, transformation enthalpy and activation energy over a wide range of temperature [2]. In addition, the high thermal conductivity as well as the temperature at which transformations occurs in most amorphous alloys makes these transformations particularly suited to analysis in a differential scanning calorimeter (DSC).

The study of crystallization kinetics in amorphous materials by DSC techniques has been widely discussed in the literature [3,4]. There are a large variety of mathematical treatments mostly based on the Johnson–Mehl–Avrami (JMA) transformation rate equation [5–8]. In this work the conditions of applicability of the JMA transformation rate equation to non-isothermal crystallization are established. The kinetic parameters of the above-mentioned crystallization are deduced by using the techniques of data analysis of single-scan and multiple-scan. Moreover, the present paper applies the quoted techniques to the analysis of the crystallization kinetics of the glassy alloy $\text{Ge}_{0.13}\text{Sb}_{0.23}\text{Se}_{0.64}$ and the values of the kinetic parameters thus obtained differ by about 2.5%. This fact shows the reliability and accuracy of the single-scan technique for the calculation of the quoted parameters from a continuous heating treatment. Finally, the crystalline phases corresponding to the thermal treatment of the quoted glassy alloy were identified by X-ray diffraction (XRD) measurements, using Cu K α radiation.

2. Theoretical development

The theoretical basis for interpreting DTA or DSC results is provided by the formal theory of transformation kinetics [5–7,9,10]. This theory supposes that the crystal growth rate, in general, is anisotropic, and in the case of heterogeneous nucleation induced by active substrates [11], the volume of a transformed region is then

$$v = g \prod_i \int_0^t u_i(t') dt' \quad (1)$$

where the expression $\prod_i \int_0^t u_i(t') dt'$ condenses the product of the integrals corresponding to the values of the above quoted subscript i , and g is a geometric factor, which depends on the dimensionality and shape of the crystal growth, and therefore its dimension equation can be expressed as

$$[g] = [L]^{3-i}, \quad ([L] \text{ is the length}).$$

When the crystal growth is isotropic, $u_i = u$, an assumption which is in agreement with the experimental evidence, since in many transformation the reaction products grow approximately as spherical nodules [11], Eq. (1) can be written as

$$v = g \left[\int_0^t u(t') dt' \right]^m \quad (2)$$

where m is an exponent related to dimensionality of the crystal growth.

Defining an extended volume of transformed material [11–14], the above-mentioned elemental volume, dV_e , is expressed as

$$dV_e = v dN' = g \left[\int_0^t u(t') dt' \right]^m dN' \quad (3)$$

dN' being the elemental number of nuclei existing in the sample.

To obtain a general kinetic equation for the true volume transformed, the mutual interference of regions growing from separated nuclei must be considered. According to Avrami's model [5–7] it is now possible to find the following relationship between the extended volume, $V_e(t)$, and the actual volume, $V_b(t)$:

$$dV_b(t) = \left(1 - \frac{V_b(t)}{V} \right) dV_e(t) \quad (4)$$

V being the volume of the whole assembly, and where both V_b and V_e change with time.

The general solution of the preceding differential equation is given as

$$\frac{V_b(t)}{V} = 1 - \exp\left(\frac{-V_e(t)}{V}\right) \quad (5)$$

In terms of the quoted general Avrami formulation to analyse particular models of crystallization is equivalent to assume different $V_e(t)$ dependences [15].

Thus, in the case of a grained glass sample it can be supposed that on the free surface of the material exists a concentration, C_n , of nuclei growing with a velocity u . These nuclei are formed at lower temperatures in the process of temperature rise, mainly under the catalytic effect of foreign substrates, dust, active sites, etc.

By integrating Eq. (3) the extended volume is obtained as

$$V_e(t) = gN \left[\int_0^t u(t') dt' \right]^m \quad (6)$$

Given that the material is grained the number of nuclei is written as $N = C_n S_s$ (S_s being the total surface area of the sample). This area can be expressed as the multiplication of the grain number, $N_g = V/V_g$ ($V_g = (4\pi/3)R_g^3$ is the volume of grain) by the surface area of a glass grain, $S_g = 4\pi R_g^2$. Bearing in mind these assumptions, Eq. (6) becomes

$$V_e(t) = C_n \frac{3V}{R_g} g \left[\int_0^t u(t') dt' \right]^m \quad (7)$$

where the kinetic exponent is $n = m$, since the case of “site saturation” [16] has been considered.

In the case of linear growth, this is, u independent of the time, and considering the initial stages of crystallization when the growing crystallites do not interact, yet three-dimensional growth is to be expected, and the extended volume is given

as

$$V_e(t) = C_n \frac{3V}{R_g} g u^3 t^3 \quad (8)$$

This three-dimensional growth of the surface nucleated crystallization centres becomes practically impossible, when the diameter, d_m , and the surface concentration of the corresponding nuclei fulfil the following relationships

$$C_n = \frac{N_n}{S_g} = \frac{1}{S_m} = \frac{4}{\pi d_m^2} \quad (9)$$

where N_n is the number of nuclei in the surface of a grain and S_m the maximum meridian section of each nucleus (see Fig. 1). Accordingly, the time elapsed during the quoted three-dimensional growth is expressed as

$$t_{3-D} = \frac{d_m}{2u} = \left(u\sqrt{\pi C_n}\right)^{-1} \quad (10)$$

Bearing in mind Eqs. (5) and (8) the volume fraction transformed with three-dimensional growth may be written as

$$x(t) = 1 - \exp\left[-\frac{A_{3-D}}{R_g} u^3 t^3\right] \quad (11)$$

where $A_{3-D} = 8d_m^{-2}$ if it is assumed that the geometric factor of a hemisphere is $g = 2\pi/3$. It should be noted that for glass semolina samples for which the condition $(R_g/u) \rightarrow 0$ is fulfilled, according to Eq. (11), the fraction transformed after time t_{3-D} is $x(t_{3-D}) \approx 1$.

After an intermediate period of crystal selection, radial growth of a colony of needle-like crystallites, perpendicular to the surface of the grains is usually observed [15]. In this stage of the process with one-dimensional growth, the geometric factor is $g = \pi d_m^2/4$ and the volume fraction crystallized is expressed, according to Eqs. (5) and (7), by means of the following expression

$$x(t) = 1 - \exp[-x_e(t)] = 1 - \exp\left[-\frac{A_{1-D}}{R_g} ut\right] \quad (12)$$

where $A_{1-D} = 3$ and the kinetic exponent is $n = 1$. It should be noted that for this law of $x_e(t)$, at $x_e(t) \ll 1$ and according to Eq. (12), the volume fraction transformed may be written as

$$x(t) \approx \frac{3}{R_g} ut \quad (13)$$

i.e. the same approximative solution as this one following from the classical Jander law [17]

$$x(t) = 1 - \left(1 - \frac{ut}{R_g}\right)^3 \approx \frac{3}{R_g} ut \quad (14)$$

for $(ut/R_g) \rightarrow 0$.

It follows also from Eqs. (11) and (12) that at constant temperature and the same time, t_z , the logarithmic forms of the fractions $x(t_z)$, which crystallize in glass semolina samples with different grain radii should give straight lines,

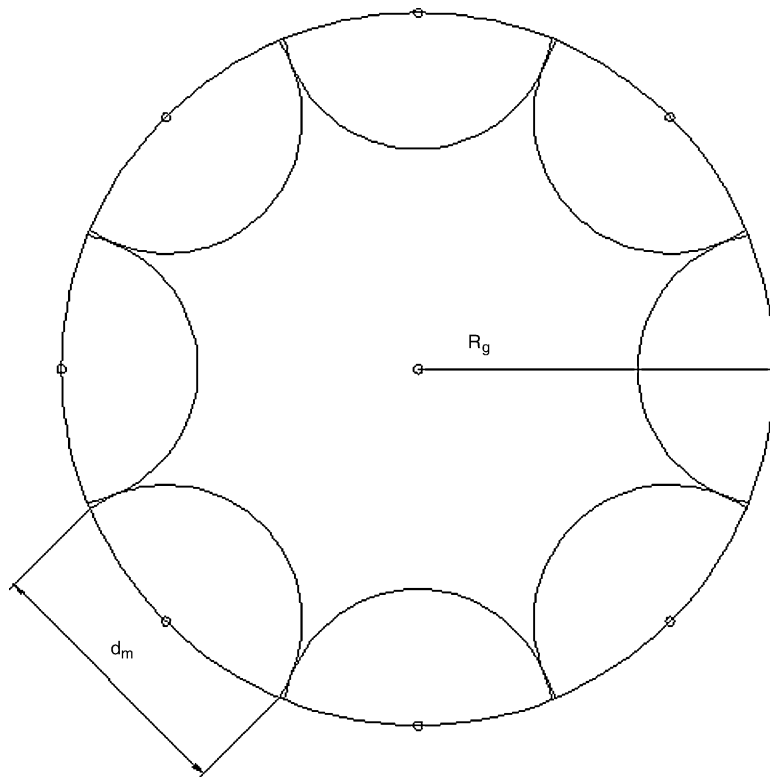


Fig. 1. An illustration of the determination of the time t_{3-D} , by means of Eqs. (9) and (10), during which crystalline nuclei with concentration C_n on the surface of the glass grain grow as caps into the bulk of this grain, where d_m is the size of a cap and R_g the glass grain radius.

$\ln[1 - x(t_z)]$ versus R_g^{-1} or $x(t_z)$ versus R_g^{-1} for small x values if $\ln[1 - x(t_z)]$ is expanded as a series and only the first term is taken.

It should be noted that Eqs. (11) and (12) may be expressed by the more general relationships, which reflects a n -dimensional growth

$$x(t) = 1 - \exp \left[- \left[(A_{n-D}/R_g)^{1/n} ut \right]^n \right] \quad (15)$$

where A_{n-D} is a factor, which depends on the surface concentration and the dimensionality of the crystal growth, since the above-mentioned case of “site saturation” ($n = m$) has been considered. Note that the dimension equation of the quoted factor can be expressed as

$$[A_{n-D}] = [L]^{1-n}$$

Eq. (15) can be taken as a detailed specific case of the JMA transformation equation

$$x(t) = 1 - \exp[-(Kt)^n] \quad (16)$$

where the reaction rate constant, K , is a function of temperature, because it depends on the crystal growth rate.

The isothermal transformation rate, dx/dt , can be easily determined from Eq. (16) taking the derivative with respect to time and substituting into the resulting expression the explicit relationship between x and t given by Eq. (16) to yield

$$\frac{dx}{dt} = nK(1-x)[- \ln(1-x)]^{(n-1)/n} \quad (17)$$

This equation is sometimes referred to as the JMA transformation rate equation.

2.1. Evaluation of the Johnson–Mehl–Avrami transformation rate equation under conditions of continuous heating

It was suggested by Henderson [18] in a notable paper that Eq. (17) as developed by Johnson, Mehl and Avrami is based on the following important assumptions:

1. isothermal transformation conditions;
2. spatially random nucleation;
3. growth rate of new phase dependent only on temperature and not on time.

In the past decades Eq. (17) has been applied without qualification to the analysis of non-isothermal phase transformations [19–21]. However, according to literature [22], the above-mentioned equation can be rigorously applied under non-isothermal conditions if it can be shown that the transformation rate depends only on the state variables x and T . Under this restriction, according to the literature [18], an example of a system which allows the non-isothermal application of Eq. (17) is one in which the nucleation process takes place early in the transformation and the nucleation frequency is zero thereafter, which can be referred to as “site saturation”

[16]. In addition, in the cases as the above mentioned, the reaction rate constant, K , could demonstrate a simple Arrhenius behaviour ($K = K_0 \exp(-E/RT_a)$) or a Vogel–Fulcher behaviour ($K = K_0 \exp[-E/R(T_a - T_0)]$) with respect to temperature during the crystallization process, if a sufficiently limited range of temperature for the crystallization peaks in DSC experiments is considered [23]. In these expressions of the rate constant, K_0 , is the frequency factor, E is the overall effective activation energy, R is the ideal gas constant, T_0 is a constant temperature, and T_a is the absolute temperature.

The analysis of crystallization kinetics is developed in terms of a generalized temperature parameter, T . The generalized formalism can be applied directly to either Arrhenius behaviour or Vogel–Fulcher behaviour by substituting T_a or $T_a - T_0$ for T , respectively. Considering the generalized temperature dependence for K , the kinetic parameters associated with the transformation process are E , n , and K_0 . The techniques of data analysis to obtain the quoted parameters can be divided into single-scan analysis and multiple-scan analysis techniques.

2.1.1. Single-scan technique

In the derivation of relationships for calculating kinetic parameters of the glass-crystal transformations by using techniques of continuous heating, a reaction rate independent of the thermal history is necessary [18]. Thus, the reaction rate is expressed as the product of two separable functions of absolute temperature and the volume fraction transformed. In these conditions Eq. (17) can be written as

$$\frac{dx}{dt} = nKf(x) = nK_0(1-x)[- \ln(1-x)]^{(n-1)/n} \times [\exp(-E/RT)] \quad (18)$$

Bearing in mind that the heating rate is $\beta = dT/dt$, Eq. (18) must be integrated by separation of variables, replacing $- \ln(1-x')$ with z' and E/RT' with y' , yielding

$$[- \ln(1-x)]^{1/n} = \frac{K_0 E}{\beta R} \int_y^\infty e^{-y'} y'^{-2} dy' = \frac{K_0 E}{\beta R} I \quad (19)$$

The integral I is not integrable in closed form and the literature [24,25] gives several series expansions for the quoted integral. Vázquez et al. [26] have developed a method to evaluate it by an alternating series, where it is possible to use only the two first terms, without making any appreciable error. The resulting expression for I is substituted into Eq. (19), whose logarithmic form, according to literature [18], gives

$$\ln[- \ln(1-x)] - 2n \ln T = - \frac{nE}{RT} + n \ln \left(\frac{RK_0}{\beta E} \right) \quad (20)$$

if it is assumed that the term $2RT/E$ is negligible in comparison to unity, since in most crystallization reactions $E/RT \gg 1$ (usually $E/RT \geq 25$) [23,27]. When n is known, a plot of $\ln[- \ln(1-x)] - 2n \ln T$ versus $1/T$ yields a straight line whose slope provides a value of the product nE . However, according to literature [28], over a temperature range of 100 K

the contribution of the term $2n \ln T$ can be ignored without causing a substantial error in the calculated slope. On the other hand, taking the logarithm of Eq. (18), according to Henderson [18], results

$$\ln \left(\frac{dx}{dt} \right) = \ln(nK_0) + \ln[f(x)] - \frac{E}{RT} \quad (21)$$

Hence when $\ln(dx/dt)$ is plotted versus $1/T$ a straight line is obtained, whose slope allows to calculate the activation energy, E , of the glass-crystal transformation, if it is assumed that for $0.25 < x < 0.75$ the function $\ln[f(x)]$ may be considered as constant [21,23]. The determination of nE and E makes it possible to directly obtain the parameter n .

For those systems in which K shows a Vogel–Fulcher temperature behaviour a determination of T_0 must also be made, according to Henderson [18]. In this case the effective activation energy, $E_{\text{eff}}(T_a)$, can be obtained by the relationship:

$$\frac{d[\ln(dx/dt)]}{dT_a^{-1}} = \frac{E_{\text{eff}}(T_a)}{R} \quad (22)$$

The derivative of the Eq. (21) with respect to T_a^{-1} leads to the expression

$$\frac{d[\ln(dx/dt)]}{dT_a^{-1}} = -\frac{E}{R} \left(\frac{T_a}{T_a - T_0} \right)^2 - nK_0 \frac{T_a^2}{\beta} \frac{df(x)}{dx} \exp \left(\frac{-E}{RT} \right)$$

Considering the negligible exponential term, and equating the resulting expression with Eq. (22), yields

$$[E_{\text{eff}}(T_a)] \left(\frac{(T_a - T_0)^2}{T_a^2} \right) \approx -E = \text{constant}$$

and measuring $E_{\text{eff}}(T_a)$ at two widely spaced temperatures T_{a1} and T_{a2} , the value of T_0 can be determined as

$$T_0 = (AT_{a1} - T_{a2})(A - 1)^{-1}$$

with $A = (T_{a2}T_{a1}^{-1}) \{ E_{\text{eff}}(T_{a1}) [E_{\text{eff}}(T_{a2})]^{-1} \}^{1/2}$. Finally, after E , n and T_0 have been determined, the frequency factor, K_0 , can be obtained by directly substituting for E and n in Eq. (18), yielding

$$K_0 = \frac{dx}{dt} \left[n [f(x)] \exp \left(\frac{-E}{RT} \right) \right]^{-1} \quad (23)$$

2.1.2. Multiple-scan technique

The single-scan analysis techniques outlined above are predicated on a detailed knowledge of the functional dependence of the transformation rate, dx/dt , on the fraction transformed, x , and the generalized temperature, T . The multiple-scan rate analysis techniques do not depend on a specific knowledge of the dependence of dx/dt on x . The procedure requires the characterization of the transformation by using several different scan rates. When this procedure is applied to the case of a JMA transformation rate equation, gen-

eralization of Eq. (16) for the treatment of continuous heating experiments is interesting. If it is assumed that the transformation products and mechanism do not change with temperature, then it is reasonable to replace Kt with $\int_0^t K[T(t')] dt'$, according to the literature [29], and Eq. (16) generalizes to

$$x = 1 - \exp \left\{ - \left[\int_0^t K(T(t')) dt' \right]^n \right\} = 1 - \exp(-I_1^n) \quad (24)$$

where $K[T(t')] = K_0 \exp(-E/RT)$ and $T(t')$ is the above-mentioned generalized temperature. The maximum transformation rate is found by making $d^2x/dt^2 = 0$, thus obtaining the relationship

$$nK_p(I_1^n)|_p = \frac{\beta E(I_1)|_p}{RT_p^2} + (n - 1)K_p \quad (25)$$

where the magnitude values which correspond to the maximum crystallization rate are denoted by subscript p . Replacing E/RT' with y' , the integral I_1 can be evaluated [26] as in Section 2.1.1, yielding an expression for $(I_1)|_p$, that when is inserted into Eq. (25) results in $(I_1)|_p = (1 - 2RT_p/nE)^{1/n}$. By equating both expressions for $(I_1)|_p$ one obtains a relationship whose logarithmic form can be written as

$$\ln \left(\frac{T_p^2}{\beta} \right) + \ln \left(\frac{K_0 R}{E} \right) - \left(\frac{E}{RT_p} \right) \approx \frac{2RT_p}{E} \left[1 - \left(\frac{1}{n^2} \right) \right] \quad (26)$$

where the function $\ln(1 - v)$ with $v = 2RT_p/nE$ or $v = 2RT_p/E$ is expanded as a series and has been taken only the first term of itself.

Note that, for most crystallization reactions, the right hand side (RHS) of Eq. (26) is generally negligible in comparison to the individual terms on the left-hand side for common heating rates ($\leq 100 \text{ K min}^{-1}$), thus for $n > 1$ and $E/RT_p > 25$ the error introduced in the value of E/R is less than 1%. Eq. (26) serves to determine the activation energy, E , and the frequency factor, K_0 , from the slope and intercept, respectively, of the $\ln(T_p^2/\beta)$ versus $1/T_p$ plot.

Finally, it should be noted that Eq. (26) with RHS = 0 is obtained, considering that $2RT_p/E \ll 1$, according to the literature [23], and therefore $(I_1)|_p = 1$. Thus, deriving Eq. (24) with respect to time and considering the expression for K_p when $(I_1)|_p = 1$ it is possible to obtain

$$n = \frac{dx}{dt} \Big|_p RT_p^2 (0.37\beta E)^{-1} \quad (27)$$

which permits us to calculate the kinetic exponent n in a set of exotherms taken at different heating rates and the corresponding mean value represents the most probable value of the kinetic exponent of the transformation process.

3. Experimental

The semiconducting $\text{Ge}_{0.13}\text{Sb}_{0.23}\text{Se}_{0.64}$ glassy was made in bulk form, from their components of 99.999% purity, which were pulverized to less than $64\ \mu\text{m}$, mixed in adequate proportions, and introduced into quartz ampoules. The ampoules were subjected to an alternating process of filling and vacuuming of inert gas, in order to ensure the absence of oxygen inside. This ended with a final vacuuming process of up to 10^{-2} Pa, and sealing with an oxyacetylene burner. The ampoules were put into a furnace at 1223 K for 44 h, turning at 1/3 rpm, in order to ensure the homogeneity of the molten material, and then quenched in water with ice to avoid the crystallization. The capsules containing the samples were then put into a mixture of hydrofluoric acid and hydrogen peroxide in order to corrode the quartz and make it easier to extract the alloy. The glassy state of the material was confirmed by a diffractometric X-ray scan, in a Siemens D500 diffractometer, showing an absence of the peaks which are characteristic of crystalline phases. The homogeneity and composition of the samples were verified through scanning electron microscopy (SEM) in a Jeol, scanning microscope JSM-820. The calorimetric measurements were carried out in a Perkin-Elmer DSC7 differential scanning calorimeter with an accuracy of ± 0.1 K. A constant $60\ \text{ml}\ \text{min}^{-1}$ flow of nitrogen was maintained in order to provide a constant thermal blanket within the DSC cell, thus eliminating thermal gradients and ensuring the validity of the applied calibration standard from sample to sample. Moreover, the nitrogen purge allows to expel the gases emitted by the reaction, which are highly corrosive to the sensory equipment installed in the DSC furnace. The calorimeter was calibrated, for each heating rate, using the well-known melting temperatures and melting enthalpies of high purity zinc and indium supplied with the instrument. The analysed samples were pulverized (particle size around $40\ \mu\text{m}$), crimped into aluminium pans, and their masses were kept about 20 mg. An empty aluminium pan was used as reference. The crystallization experiments were carried out through continuous heating at rates, β , of 2, 4, 8, 16, 32 and $64\ \text{K}\ \text{min}^{-1}$. The glass transition temperature was considered as a temperature corresponding to the inflection point of the lambda-like trace on the DSC scan, as shown in Fig. 2.

The crystallized fraction, x , at any temperature, T , is given by $x = A_T/A$, where A is the total area of the exotherm between the temperature T_i where the crystallization is just beginning and the temperature T_f where the crystallization is completed, and A_T is the area between the initial temperature and a generic temperature T (see Fig. 2). With the aim of investigating the phases into which samples crystallize, diffractograms of the material transformed during thermal process were obtained. The experiments were performed with a Philips diffractometer (type PW1830). The patterns were run with Cu as target and Ni as filter ($\lambda = 1.542\ \text{\AA}$) at 40 kV and 40 mA, with a scanning speed of $0.1^\circ\ \text{s}^{-1}$.

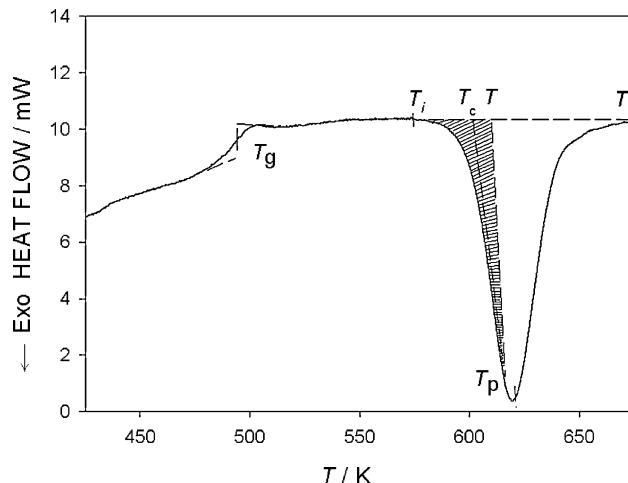


Fig. 2. Typical DSC trace of $\text{Ge}_{0.13}\text{Sb}_{0.23}\text{Se}_{0.64}$ glassy alloy at a heating rate of $32\ \text{K}\ \text{min}^{-1}$. The hatched area shows A_T , the area between T_i and T_f .

4. Results and discussion

The typical DSC curve of $\text{Ge}_{0.13}\text{Sb}_{0.23}\text{Se}_{0.64}$ semiconductor glass obtained at a heating rate of $32\ \text{K}\ \text{min}^{-1}$ and plotted in Fig. 2 shows three characteristic phenomena which are resolved in the temperature region studied. The first one ($T = 493\ \text{K}$) corresponds to the glass transition temperature T_g , the second ($T = 601\ \text{K}$) to the extrapolated onset crystallization temperature T_c , and the third ($T = 619\ \text{K}$) to the peak temperature of crystallization T_p of the above-mentioned semiconductor glass. The quoted DSC trace shows the typical behaviour of a glass-crystal transformation. The thermograms for the different heating rates, β , quoted in Section 3, show values T_g , T_c and T_p which increase with increasing β , a property which has been widely quoted in the literature [30,31].

4.1. Crystallization

The analysis of the crystallization kinetics is related with the knowledge of the reaction rate constant as a function of the temperature. It should be noted that the assumption of an Arrhenius type temperature dependence for the quoted constant, as many authors have considered in the last decades, is a very rough approximation [23]. Therefore, in the present work it is considered that the rate constant is a function of the temperature under more general conditions [23,32]. In order for these conditions to hold, according to literature [23], one of the following two sets of hypotheses should apply:

- (i) The crystal growth rate, u , can depend on the temperature through of the viscosity, when, e.g., the crystal growth takes place by a normal growth mechanism; and over the temperature range where the thermoanalytical measurements are carried out, the nucleation rate is negligible (i.e., the condition of "site saturation").

Table 1
The characteristic temperatures and enthalpies of the crystallization processes of alloy Ge_{0.13}Sb_{0.23}Se_{0.64}

Parameter	Experimental value
T_g (K)	474.0–499.2
T_i (K)	558.7–599.7
T_p (K)	581.1–631.3
ΔT (K)	42.0–56.7
ΔH (mJ mg ⁻¹)	25.7–32.0

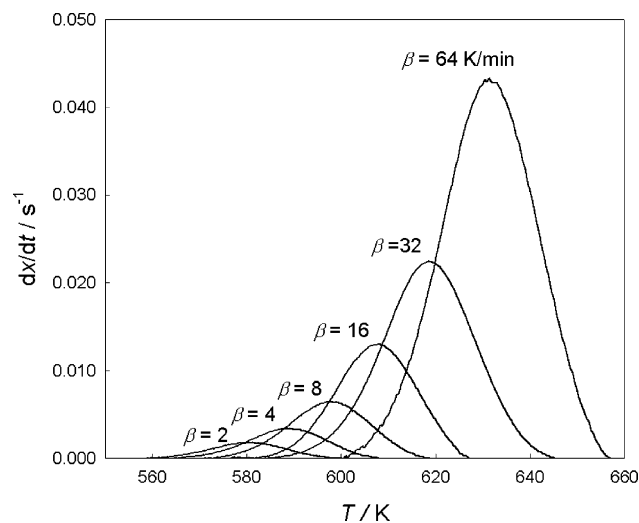


Fig. 3. Crystallization rate vs. temperature of the exothermal peaks, at different heating rates.

(ii) Both the crystal growth and the nucleation, which depend on the temperature under general conditions, occur simultaneously [33].

In this work the first set of conditions is assumed in order to apply the JMA equation under regime of continuous heating. From this point of view, the crystallization kinetics of the Ge_{0.13}Sb_{0.23}Se_{0.64} alloy has been analysed by using the calorimetric techniques of single-scan and multiple-scan.

With the aim of analysing the above-mentioned kinetics, the variation intervals of the quantities described by the thermograms for the different heating rates, quoted in Section 3 are obtained and given in Table 1, where T_i and T_p are the temperatures at which crystallization begins and that corresponding to the maximum crystallization rate, respectively, and ΔT is the width of the peak. The crystallization enthalpy, ΔH , is also determined for each heating rate.

The area under the DSC curve is directly proportional to the total amount of material transformed. The ratio between the ordinates and the total area of the peak gives the corresponding transformation rates, which make it possible to plot the curves of the exothermal peaks represented in Fig. 3. It may be observed that the $(dx/dt)_p$ values increase in the same proportion as the heating rate, a property which has been widely discussed in the literature [30,31].

The single-scan technique was applied to several sets of experimental data (Table 2) obtained for all heating rates,

Table 2
Kinetic parameters found for the crystallization of the Ge_{0.13}Sb_{0.23}Se_{0.64} alloy by using the single-scan and multiple-scan techniques

β (K min ⁻¹)	Single-scan					Multiple-scan						
	Interval											
	T (K)	x	$10^3(dx/dt)$ (s ⁻¹)	nE (kJ mol ⁻¹)	E (kJ mol ⁻¹)	n	K_0 (s ⁻¹)	T_p (K)	$10^3(dx/dt)_p$ (s ⁻¹)	n	E (kJ mol ⁻¹)	K_0 (s ⁻¹)
2	572.4–579.7	0.1539–0.3783	1.03–1.73	397.10	200.56	1.98	2.17×10^{15}	581.1	1.81	2.08		
4	580.8–588.0	0.1733–0.4060	2.06–3.42	399.27	198.63	2.01	1.53×10^{15}	588.0	3.42	2.01		
8	588.8–596.1	0.1592–0.3831	3.71–6.28	411.81	206.95	1.99	11.50×10^{15}	597.5	6.45	1.96	199.43	1.81×10^{15}
16	598.6–607.2	0.1501–0.4023	7.32–12.92	407.00	204.53	1.99	5.37×10^{15}	607.7	12.99	2.04		
32	608.3–617.4	0.1520–0.4166	12.40–22.19	408.56	203.36	2.01	3.72×10^{15}	618.3	22.44	1.82		
64	618.7–631.7	0.1083–0.4367	19.55–42.96	404.92	200.43	2.02	1.76×10^{15}	631.3	43.28	1.83		

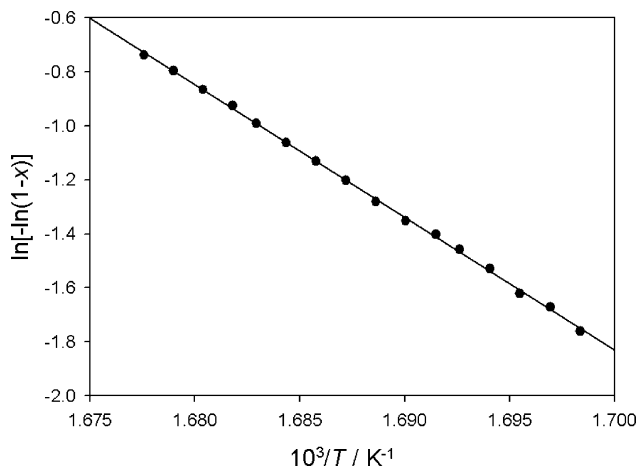


Fig. 4. Variation of $\ln[-\ln(1-x)]$ with $1/T$ for a heating rate of 8 K min^{-1} .

quoted in Section 3, and the results for nE from Eq. (20), E from Eq. (21), n derived there from and K_0 are included in Table 2. The mean values for these parameters are: $\langle E \rangle = 202.3 \text{ kJ mol}^{-1}$, $\langle n \rangle = 2$ and $\langle K_0 \rangle = 4.34 \times 10^{15} \text{ s}^{-1}$. To illustrate the above-mentioned technique, Fig. 4 shows the plots of $\ln[-\ln(1-x)]$ versus $1/T$ for $\beta = 8 \text{ K min}^{-1}$, together with the corresponding straight regression line, while the plots of $\ln(dx/dt)$ versus $1/T$ with the straight regression line carried out, are shown in Fig. 5.

On the other hand, the multiple-scan technique, which allows E to be quickly evaluated, has been used to analyse the crystallization kinetics of the semiconducting $\text{Ge}_{0.13}\text{Sb}_{0.23}\text{Se}_{0.64}$ alloy. The plots of $\ln(T_p^2/\beta)$ versus $1/T_p$ at each heating rate, and the straight regression line carried out are shown in Fig. 6. The results for E and K_0 from Eq. (26) are given in Table 2.

By using the values of the maximum crystallization rate, and the temperatures, which correspond to the quoted maximum values, given in Table 2, it is possible to obtain, through the Eq. (27), the kinetic exponent of the process corresponding to each of experimental heating rates. The values of the

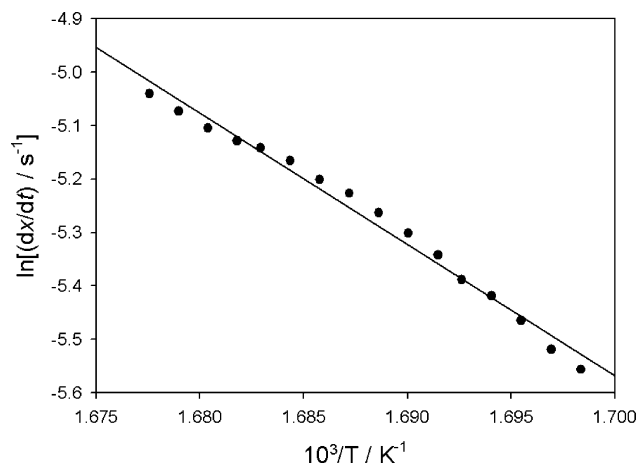


Fig. 5. Experimental plots of $\ln(dx/dt)$ vs. $1/T$ and straight regression line of the $\text{Ge}_{0.13}\text{Sb}_{0.23}\text{Se}_{0.64}$ alloy.

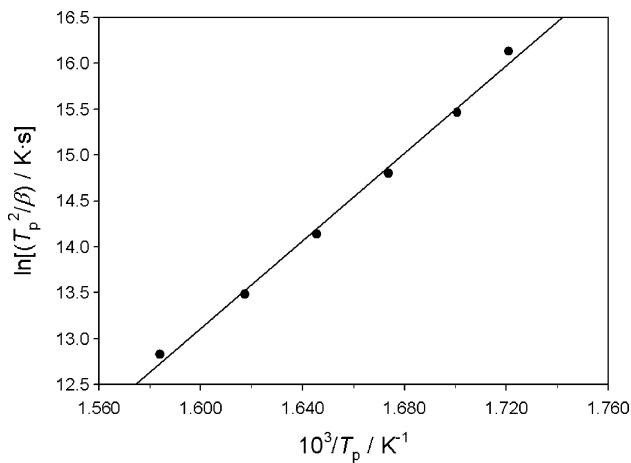


Fig. 6. Plots of $\ln(T_p^2/\beta)$ vs. $1/T_p$ of the analysed material (β in K s^{-1}).

n -parameter are also shown in Table 2. Bearing in mind that the calorimetric analysis is an indirect method which makes it possible to obtain mean values for the parameters that control the kinetics of a reaction, the corresponding mean value, $\langle n \rangle = 1.96$, has been calculated.

With the aim of correctly analysing the reliability of the single-scan technique, when calculating kinetic parameters in non-isothermal crystallization processes, the above parameters E , n and $\ln K_0$, calculated by means of the above-mentioned technique, are compared with its values obtained through the multiple-scan technique, Table 2, finding that the error between them for the less accurate parameter is less than 2.5%. This result is in agreement with the literature [21], where is shown that for $(n-1)/n = 0.6$ in the range of $0.2 < x < 0.4$ it results in an error of 7% in the calculated slope, E/R , an error acceptable in most crystallization reactions.

Considering that the crystallization process of the studied material is basically a growth of the pre-existing nuclei in the as-quenched glass, “site saturation”, it is possible to affirm, according to the literature [15], that the kinetic exponent, n , in the case of crystallization of finely grained samples has a physical meaning, which is determined by the ratio of growth rate/radius of sample grains, as it is deduced from Eqs. (11) and (12). It should be noted that in Eq. (11) of three-dimensional growth, $n = 3$, the ratio $u/R_g \rightarrow \infty$, whereas in Eq. (12) of one-dimensional growth, $n = 1$, the ratio $u/R_g \rightarrow 0$. This fact shows that in grained glass samples the kinetic exponent decreases with the increasing grain radius, which is in agreement with the literature [15,34].

5. Identification of the crystalline phases

Taking into account the crystallization exothermal peaks shown by the semiconducting $\text{Ge}_{0.13}\text{Sb}_{0.23}\text{Se}_{0.64}$ alloy, it is recommended to try to identify the possible phases that crystallize during the thermal treatment applied to the samples by means of adequate XRD measurements. For this purpose

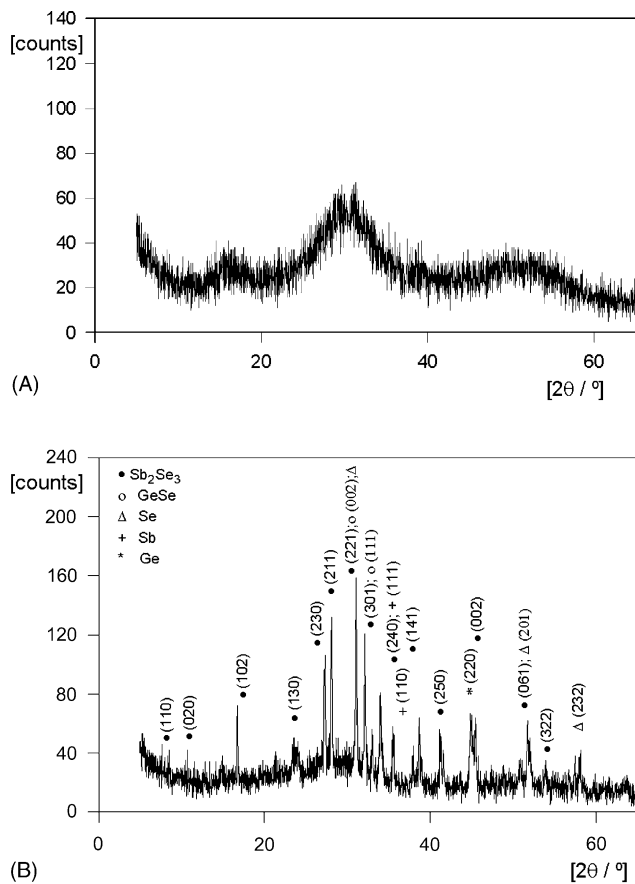


Fig. 7. (A) Diffractogram of the amorphous $\text{Ge}_{0.13}\text{Sb}_{0.23}\text{Se}_{0.64}$ alloy. (B) Diffraction peaks of the quoted alloy crystallized in DSC.

in Fig. 7 we show the most relevant portions of the diffractograms for the as-quenched glass and for the material submitted to the thermal process. Fig. 7A has broad humps characteristic of the amorphous phase of the starting material at diffraction angles (2θ) between 20° and 60° . The diffractogram of the transformed material (Fig. 7B) shows that the crystallization process analysed in this work is associated with crystallites of Sb_2Se_3 and GeSe indicated with solid and open circles, respectively, together with some traces of elemental crystalline Ge , Sb and Se , remaining a residual amorphous matrix. The two quoted phases Sb_2Se_3 and GeSe crystallize in the orthorhombic system [35] with unit cells defined by $a_1 = 11.633 \text{ \AA}$, $b_1 = 11.78 \text{ \AA}$, $c_1 = 3.895 \text{ \AA}$, and $a_2 = 4.39 \text{ \AA}$, $b_2 = 3.827 \text{ \AA}$, $c_2 = 10.824 \text{ \AA}$, respectively.

6. Conclusions

The described theoretical procedure enables us to study the evolution with time of the volume fraction transformed in materials involving nucleation and crystal growth processes. This method assumes the concept of extended volume in the transformed material and the condition of random nucleation. Using these assumptions a general expression for the transformed fraction as a function of time in bulk crystal-

lization processes has been obtained. In the case of isothermal crystallization, the above-mentioned expression has been transformed in an equation, which can be taken as a specific case of the JMA transformation equation. The application of this equation to non-isothermal transformations implies restrictive conditions, as it is the case of a transformation rate which depends only on the fraction transformed and the temperature. Under this restriction the kinetic parameters have been deduced both for the single-scan technique and for the multiple-scan technique, which are applicable to constant scan rate DTA and DSC experiments on materials which obey the JMA transformation rate equation.

The above-mentioned techniques have been applied to the crystallization kinetics of the semiconducting $\text{Ge}_{0.13}\text{Sb}_{0.23}\text{Se}_{0.64}$ alloy. The difference between the obtained values for the kinetic parameters by means of both techniques is less than 2.5%. This good agreement shows the reliability of the single-scan technique for the calculation of kinetic parameters, mainly in the interval (0.2–0.5) of the volume fraction crystallized, a fact in agreement with the literature.

Acknowledgements

The authors are grateful to the Junta de Andalucía and the CICYT (Comisión Interministerial de Ciencia y Tecnología, proyect no. MAT 2001-3333) for their financial supports.

References

- [1] R. Zallen, *The Physics of Amorphous Solids*, Wiley, New York, 1983.
- [2] Z. Altounian, J.O. Strom-Olsen, in: R.D. Shull, A. Joshi (Eds.), *Thermal Analysis in Metallurgy*, The Minerals, Metals and Materials Society, Warrendale, PA, 1992, p. 155.
- [3] K.F. Kelton, *Crystal Nucleation in Liquids and Glasses*, Solid State Physics, vol. 45, Academic Press, New York, 1991.
- [4] N. Clavaguera, *J. Non-Cryst. Solids* 162 (1993) 40.
- [5] M. Avrami, *J. Chem. Phys.* 7 (1939) 1103.
- [6] M. Avrami, *J. Chem. Phys.* 8 (1940) 212.
- [7] M. Avrami, *J. Chem. Phys.* 9 (1941) 177.
- [8] M.C. Weinberg, R. Kapral, *J. Chem. Phys.* 91 (1989) 7146.
- [9] W.A. Johnson, K.F. Mehl, *Trans. Am. Inst. Mining Met. Eng.* 135 (1981) 315.
- [10] A.N. Kolmogorov, *Bull. Acad. Sci. USSR (Sci. Mater. Nat.)* 3 (1937) 3551.
- [11] J.W. Christian, *The Theory of Transformations in Metals and Alloys*, Pergamon Press, Oxford, 1975.
- [12] J. Vázquez, P. Villares, R. Jiménez-Garay, *J. Alloys Compd.* 257 (1997) 259.
- [13] P.L. López-Alemany, J. Vázquez, P. Villares, R. Jiménez-Garay, *J. Non-Cryst. Solids* 274 (2000) 249.
- [14] V.A. Shneidman, D.R. Uhlmann, *J. Chem. Phys.* 109 (1998) 186.
- [15] I. Gutzow, R. Pascova, A. Karamanov, *J. Schmelzer, J. Mater. Sci.* 33 (1998) 5265.
- [16] J.W. Cahn, *Acta Met.* 4 (1956) 572; *J.W. Cahn, Acta Met.* 4 (1956) 449.
- [17] R. Barret, *Cinetique Heterogene*, Gauthier-Villars, Paris, 1973, Chapter 5.
- [18] D.W. Henderson, *J. Non-Cryst. Solids* 30 (1979) 301.

- [19] F. Skvara, V. Satava, *J. Therm. Anal.* 2 (1970) 325.
[20] J. Sestak, *Thermochim. Acta* 3 (1971) 1.
[21] J. Sestak, *Phys. Chem. Glasses* 6 (1974) 137.
[22] T. Kemény, *Thermochim. Acta* 110 (1987) 131.
[23] H. Yinnon, D.R. Uhlmann, *J. Non-Cryst. Solids* 54 (1983) 253.
[24] P. Murray, J. White, *Trans. Br. Ceram. Soc.* 54 (1955) 204.
[25] C.D. Doyle, *Nature* 207 (1965) 290.
[26] J. Vázquez, C. Wagner, P. Villares, R. Jiménez-Garay, *Acta Mater.* 44 (1996) 4807.
[27] J. Vázquez, C. Wagner, P. Villares, R. Jiménez-Garay, *J. Non-Cryst. Solids* 235–237 (1998) 548.
[28] J. Sestak, *Thermochim. Acta* 3 (1971) 150.
[29] J. Vázquez, P.L. López-Aleman, P. Villares, R. Jiménez-Garay, *J. Alloys Compd.* 270 (1998) 179.
[30] Y.Q. Gao, W. Wang, *J. Non-Cryst. Solids* 81 (1986) 129.
[31] J. Vázquez, P.L. López-Aleman, P. Villares, R. Jiménez-Garay, *Mater. Chem. Phys.* 57 (1998) 162.
[32] M.C. Weinberg, *J. Am. Ceram. Soc.* 74 (1991) 1905.
[33] J.R. Frade, *J. Am. Ceram. Soc.* 81 (1998) 2654.
[34] I. Gutzow, *J. Cryst. Growth* 48 (1979) 569.
[35] S.A. Demboski, *Russ. J. Inorg. Chem. (Engl. Transl.)* 8 (1963) 798.